Marine Chemistry 247 (2022) 104185

Contents lists available at ScienceDirect

Marine Chemistry

journal homepage: www.elsevier.com/locate/marchem

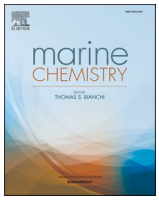

Excess pCO_2 and carbonate system geochemistry in surface seawater of the exclusive economic zone of Qatar (Arabian Gulf)

Connor Izumi [a], Jassem A. Al-Thani [b], Oguz Yigiterhan [b,**], Ebrahim Mohd A.S. Al-Ansari [b], Ponnumony Vethamony [b], Caesar Flonasca Sorino [b], Daniel B. Anderson [a], James W. Murray [a,*]

[a] School of Oceanography, University of Washington, Box 355351, Seattle, WA 98195, USA
[b] Environmental Science Center, Qatar University, P.O. Box: 2713, Doha, Qatar

ARTICLE INFO

Keywords:
pCO_2
Corals
Ocean acidification
Calcification
EEZ of Qatar
Arabian gulf

ABSTRACT

Dissolved inorganic carbon (DIC) and total alkalinity (TA) were sampled in December 2018 and May 2019 in the Exclusive Economic Zone (EEZ) of Qatar in the Arabian Gulf. pCO_2, pH and CO_3^{2-} were calculated from DIC and TA. TA, DIC and salinity increase in the Gulf due to evaporation after entering through the Strait of Hormuz. Temperature also increases. The pCO_2 in surface seawater averaged 458 ± 62 which was higher than the atmospheric value of 412 ppm. Hence, the Gulf was a source of CO_2 to the atmosphere. pCO_2 in seawater is controlled by TA relative to DIC as well as temperature and salinity. A hypothetical model calculation was used to estimate how much pCO_2 could increase in surface seawater due to various processes after entering through the Strait of Hormuz. Increases in T and S, in the absence of biogeochemical processes, would increase pCO_2 to 537 μatm, more than enough to explain the high pCO_2 observed. CO_2 is lost from the Gulf due to gas exchange, decreasing DIC, and reducing pCO_2 to 464 μatm, similar to that observed. The impact of biological processes depends on the process: calcification increases pCO_2 while net primary production decreases pCO_2. Salinity-normalized (to S = 40) total alkalinity (NTA) and dissolved inorganic carbon (NDIC) in surface seawater decrease as waters flow north from Hormuz. The slope suggests that removal of C as $CaCO_3$, organic matter (CH_2O) or gas exchange (F_{CO2}) is occurring with a ratio of $\Delta CaCO_3/(\Delta CH_2O$ or $F_{CO2}) = 1{:}2.86$. The tracer Alk*, defined as the deviation of potential alkalinity (A_P) (where $A_P = TA + 1.26\ [NO_3]$) from conservative potential alkalinity ((A_p^C), $(A_p^C = S\frac{A_p'}{S'}$ where A'$_P$ and S′ are mean values for the whole surface ocean) has values primarily determined by $CaCO_3$ precipitation and dissolution. Its values in the Gulf ranged from −50 to −310 μmol kg^{-1} implying $CaCO_3$ precipitation. The average value of ΔAlk*, the difference in Alk* between specific locations in the Qatari EEZ and the surface water entering through the Strait of Hormuz, was −130 μmol kg^{-1} which corresponded to a calcification of 65 μmol kg^{-1}. Our model calculations indicate that this would increase pCO_2 to 577 μatm. Carbonate forming plankton have not been observed in the water column suggesting that calcification occurs in corals, even though they have been severely damaged by past bleaching events. The amount of DIC removed by net primary production is small, consistent with an oligotrophic food web dominated by remineralization. It appears that the role of biological production in the water column for the control of pCO_2 is very small. The high observed pCO_2 reflects a balance between sources due to the impact of increasing T and S on the carbonate system equilibrium constants and net calcification and sinks due to CO_2 loss due to gas exchange and net primary production in surface seawater after it enters the Gulf through the Strait of Hormuz.

1. Introduction

There is growing concern that coral reefs in the Exclusive Economic Zone (EEZ) of Qatar in the Arabian (Persian) Gulf (hereafter referred to as 'Gulf') have been severely impacted by degradation of the ecosystem due to climate change and anthropogenic modifications (Burt et al., 2015). Bleaching events due to ocean warming have been well described (Burt et al., 2019), but ocean acidification (Doney et al., 2009) has

* Correspondence to: School of Oceanography, University of Washington, Box 355351, Seattle, WA 98195, USA.
** Correspondence to: Environmental Science Center, Qatar University, P.O. Box: 2713, Doha, Qatar.
E-mail addresses: oguz@qu.edu.qa (O. Yigiterhan), jmurray@uw.edu (J.W. Murray).

https://doi.org/10.1016/j.marchem.2022.104185
Received 8 February 2022; Received in revised form 17 October 2022; Accepted 27 October 2022
Available online 5 November 2022
0304-4203/Published by Elsevier B.V. This is an open access article under the CC BY-NC-ND license (http://creativecommons.org/licenses/by-nc-nd/4.0/).

received little attention (Uddin et al., 2012). Little is known about the aqueous carbonate system geochemistry in this region since a 1977 study by Brewer and Dyrssen (1985). Reefs cover a relatively small area (Rezai et al., 2004) but they are the region's biological storehouse (Abdel-Moati, 2006; Vaughan et al., 2019). Historically, the countries bordering the Gulf drew on pearl oyster beds and coral reefs as a large part of their economy and cultural heritage. The World-Wide Fund for Nature (WWF) has identified the Gulf as part of a Global 200 Ecoregion - one of 43 priority marine ecosystems worldwide (Spalding et al., 2007).

The Gulf is a semi-enclosed marginal sea with an area of 240,000 km^2 and mean depth of 35 m (Kampf and Sadrinesab, 2006; Vaughan et al., 2019). The deeper areas of the Gulf (~80 m) are located along the Iranian coast, whereas broad, shallow regions with depths <35 m are found along the coast of Qatar and the Arabian Peninsula. The seawater in the Gulf exchanges freely with the Gulf of Oman in the Arabian Sea through the Strait of Hormuz, which is 56 km wide and has a maximum depth of 100 m. The circulation in the Gulf is characterized as reverse estuarine. Lower salinity (S = ~36.5) seawater enters at the surface through the Strait of Hormuz. The climate of this regions is very hot and dry and evaporation is estimated to be ~200 cm yr^{-1} for the central region of the Gulf (Al Ansari et al., 2015). Thus, the salinity and density increase due to evaporation as seawater flows to the north from the Strait. Higher salinity seawater (S ≥ 40) exits at depth as return flow through the Strait (Brewer and Dyrssen, 1985). Due to geostrophy, the inflow of Indian Ocean Surface Water (IOSW) follows the Iranian coastline, whereas the denser bottom outflow follows the Arabian coast (Brewer and Dyrssen, 1985). The total volume of the Gulf is ~8600 km^3 and the flux of the deep outflow through Hormuz is about 6620 km^3 y^{-1}. Therefore, the residence time of seawater in the Gulf is 1.3 years (Sheppard et al., 2010).

The water column is well-mixed in winter, driven by shear associated with tidal forces and winds, especially along the shallow Arabian coast (Alosairi et al., 2011). Stratification occurs in summer due to surface warming. Previous studies have shown that inorganic nutrient concentrations are normally very low (e.g., <0.5 μmol kg^{-1} NO_3^-) in surface water and can be as high as 4.5 μmol kg^{-1} in the hypoxic deeper water (Quigg et al., 2013). As a result, the ecosystem is oligotrophic and nitrate limited (Quigg et al., 2013).

Concentrations of carbonate system parameters (DIC and TA) in the surface waters reflect a balance between the inputs through the Strait, enrichment due to evaporation, fluxes due to air-sea gas exchange and biological processes (net primary production and net calcification). The carbonate system chemistry in the Gulf was first sampled in 1977 (Brewer and Dyrssen, 1985). Their study showed that surface water enters the Gulf from the Arabian Sea with high concentrations of dissolved inorganic carbon (DIC)(~2075 μmol kg^{-1}) and total alkalinity (TA) (~2380 μeq kg^{-1}). These high concentrations reflect upwelling from the shallow oxygen minimum in the Arabian Sea. As the water flows northward, DIC and TA increase but salinity-normalized DIC (NDIC) and alkalinity (NTA) decrease. The decrease in NDIC and NTA can be used to determine the relative importance of carbon removal by net $CaCO_3$ formation versus net primary production. As the surface seawater flows northward, the partial pressure of carbon dioxide (pCO_2) reflects changes in the carbonic acid equilibria due to increasing T and S, net primary production, net calcification, and CO_2 lost to the atmosphere by gas exchange. At the time of Brewer and Dyrssen's study in 1977, the Arabian Gulf was degassing CO_2 to the atmosphere. Now, 40 years have passed and the gradients and fluxes may have changed. Because data regarding the progress of ocean acidification in the EEZ of Qatar are sparse, an international collaboration between Qatar University (QU) and the University of Washington (UW) provided an opportunity to generate more recent data.

The goal of this study was to assess the status of the ocean carbonate system in the Exclusive Economic Zone of Qatar in the Arabian Gulf with respect to present and future impacts by ocean acidification. We use distributions of DIC and TA to determine the relative importance of organic matter production and $CaCO_3$ formation as sinks and sources of carbon and to determine pCO_2 in surface seawater.

2. Materials and methods

2.1. Field sampling

Water column sampling was conducted, using, rosette-mounted, 10-L PVC Niskin bottles. Samples were collected on December 5, 2018 (winter) and May 18, 2019 (summer) in the EEZ of Qatar on the R/V Janan (Fig. 1). Seawater samples and hydrographic data were collected at seven stations (stations 1C, 2C, 3C, 4C, 5C, 6B, 6C) along a transect from the central east coast of Qatar across the Qatari Exclusive Economic Zone (EEZ). Stations were chosen to be nearly perpendicular to the major axis of the Gulf to capture main regional hydrographic features across the EEZ. The transect provided a reasonable representation of hydrographic distributions across the wider part of the Gulf. Vertical profiles were collected with one surface sample, one bottom sample, and 1 to 3 mid-depth samples at deeper stations 2C, 4C, 6B, and 6C.

Samples for DIC and TA were collected in 300 mL Wheaton BOD glass bottles with ground glass stoppers. Samples were poisoned with 150 μL $HgCl_2$ (0.05% by volume) after collection, to prevent biological activity, then sealed immediately, using Apiezon-M grease, to prevent loss of CO_2. Dissolved oxygen samples were taken directly from Niskin bottles in 300 mL Wheaton BOD bottles and immediately inoculated with manganese chloride and potassium iodide solutions before analysis onboard. One-liter samples of seawater for Chlorophyll-a (Chl-a) were filtered on 0.45 μm filters (Millipore), which were folded and stored at −20 °C.

2.2. Analyses

During both cruises, hydrographic properties (temperature and practical salinity (S_p)) were measured using a calibrated Sea-Bird Scientific, SBE 9 mounted on a SeaBird rosette (Talley et al., 2011). Samples were taken directly from the Niskin bottles and analyzed for dissolved oxygen within a few hours of collection using the Winkler titrimetric method (Carpenter, 1965) to ±0.4 μmol kg^{-1}. Samples were analyzed for Chlorophyll-a using the classic technique of Lorenzen (1967), with a detection limit of 0.02 μg/L and precision of ±5% (Strickland and Parsons, 1972).

We measured two commonly measured carbonate chemistry parameters, TA and DIC. These are the primary capacity factors of the carbonate system (Stumm and Morgan, 1995). Being capacity factors means that they behave conservatively during mixing, in the absence of non-conservative fluxes such as gas exchange (DIC) and biological processes (TA and DIC). DIC and TA may not be the most precise pair of variables to calculate pH, pCO_2 and the carbonate ion concentration (Orr et al., 2018) but they were the most convenient parameters for us to measure on samples collected in the Gulf and shipped to the University of Washington for analyses.

Samples were analyzed in Dr. Alex Gagnon's carbonate chemistry laboratory at the University of Washington. Analyses were completed within one month of collection. Carbonate system measurements followed the methods of Dickson et al. (2007). Briefly, TA (μmol kg^{-1}) was determined through open-cell automated titration (876 Dosimat plus, Metrohm AG) with a 0.1 M hydrochloric acid (HCl) + 0.6 M sodium chloride (NaCl) solution. DIC (μmol kg^{-1}) was obtained through coulometric determination (VINDTA 3D, Marianda with UIC coulometer). Certified reference materials (CRM) for TA and DIC, obtained from Andrew Dickson's lab (Scripps Institution of Oceanography), were run in conjunction with seawater samples to ensure analytical accuracy. Based on repeated measurements of an internal laboratory standard and CRM, long term analytical precisions for DIC and TA were ± 3.7 μmol kg^{-1} (2σ std. dev.) and ± 4.3 μmol kg^{-1} (2σ std. dev.), respectively (Bolden et al., 2019).

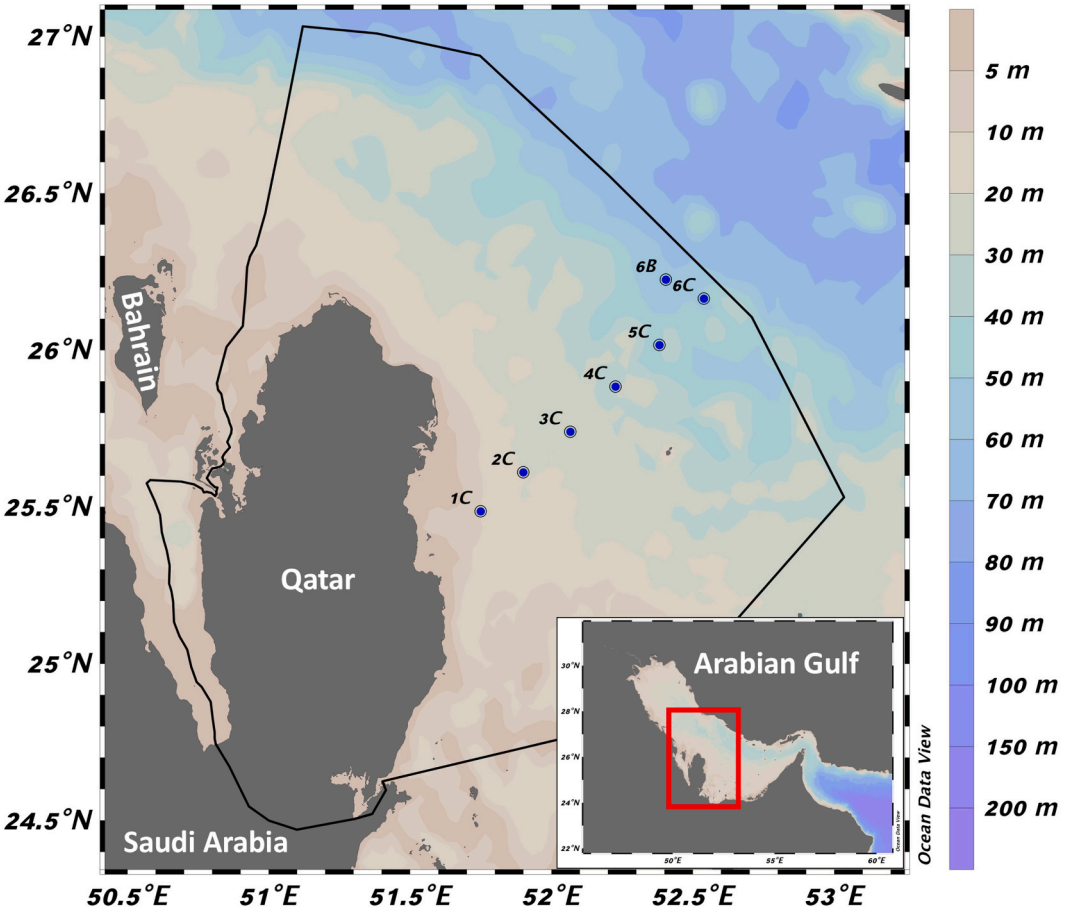

Fig. 1. Station locations sampled in December 2018 and May 2019 in the Exclusive Economic Zone (EEZ) of Qatar in the Arabian Gulf. The black line shows the boundary of the EEZ. The insert shows the location of Qatar in the Arabian Gulf. The water depths are calibrated using the color bar on the right.

pCO_2, pH (total H^+ ion scale) and $[CO_3^{2-}]$ were calculated from DIC and TA using CO2SYS v2.1 for Microsoft Excel (Pierrot et al., 2006) with carbonate equilibrium constants from Millero (2010), borate alkalinity calculated using the boron / chlorinity (salinity) relationship provided by Uppström (1974) and bisulfate dissociation constant from Dickson (1990). The uncertainties for pCO_2, pH and $[CO_3^{2-}]$, calculated from DIC and TA, were ± 10 μatm, ±0.01 and ± 0.1 μmol kg^{-1} respectively (Orr et al., 2018). Where necessary, TA, and DIC values were salinity-normalized (NTA, NDIC) to a reference salinity of 40.0 to account for evaporation. As there are no significant freshwater contributions from rivers or groundwater in this region, the normalization method of Friis et al. (2003) was not necessary.

2.3. The tracer Alk*

Carter et al. (2014) defined Alk* as the deviation of potential alkalinity from conservative potential alkalinity:

$$Alk^* = A_P - A_p^C \quad (1)$$

This tracer has values primarily determined by $CaCO_3$ precipitation and dissolution.

Potential Alkalinity (A_P) is defined as:

$$A_P = TA + 1.26\,[NO_3] \quad (2)$$

where $[NO_3]$ is the concentration of nitrate (μmol kg^{-1}) and the coefficient 1.26 is an empirical relationship that includes the combined acidifying effect of nitrate, sulfate and phosphate (Brewer and Goldman, 1976; Kanamori and Ikegami, 1982). Though derived for the North Pacific, the coefficient for NO_3 in the equation appears to be globally applicable (Wolf-Gladrow et al., 2007) and was previously applied to the Arabian Gulf by Carter et al. (2014). To remove the dependence on salinity, a background concentration, conservative potential alkalinity (A_p^C), is calculated as:

$$A_p^C = S\,\frac{A_p'}{S'} = S \text{ x } 66.40\ \mu mol\ kg^{-1} \quad (3)$$

where A'$_P$ and S′ are mean values for the whole surface ocean. Though our data are from a coastal region, we assume this equation is valid as fresh water input is negligible.

3. Results

The hydrographic (T, S_p, O_2) and carbonate system (DIC, TA) data collected at all stations and depths are given in Table 1. Calculated pCO_{2calc}, pH_{calc} and the saturation state for aragonite (Ω_{Ar}) are also given in Table 1. The means and standard deviations for all samples on the individual dates are given for each cruise. The grand averages for the combined data sets were DIC = 2180 ± 40 μmol kg^{-1}, TA = 2532 ± 30 μmol kg^{-1}, pH = 8.02 ± 0.05 and pCO_2 = 457 ± 61 μatm (Table 2). Based on the *t*-test, the means of TA, pCO_2 and pH for the whole data set differed significantly between seasons ($p < 0.01$), due to increases in concentrations with water depth at the deepest, offshore stations in May 2019. The DIC means did not differ between seasons ($p > 0.05$), and there were no statistical seasonal differences for either TA or DIC in the surface samples, hence the surface data (<2 m) from these two cruises were combined for the discussion. In spite of these small differences, the grand average for all samples and the surface samples agreed well for DIC, TA, pCO_2, pH_{calc}, Ω_{Ar} and S_p (Table 2) indicating that the water

Table 1
Water column hydrographical (Temperature and Salinity) and carbonate system parameters from December 2018 and May 2019. The units for O_2, DIC and TA are all μmol kg^{-1}. The unit for pCO_2 is μatm. The carbonate system equilibrium constants used to calculate pH_{calc} and Ω_{Ar} were from Millero (2010).

Data from December 2018									
Station	Depth	Temperature	Salinity	O2	DIC	TA	pCO2	pHcalc	Ω Ar
	m	°C		μmol kg^{-1}	μmol kg^{-1}	μmol kg^{-1}	μatm		
1C	1.8	24.621	40.983	197	2065	2426	390.5	8.055	3.78
1C	10.3	24.458	40.994	196	2085	2415	439.8	8.013	3.48
2C	1.5	25.550	40.766	198	2128	2517	387.4	8.071	4.14
2C	22.3	24.900	40.855	191	2134	2514	391.9	8.067	4.03
3C	1.4	26.683	40.641	201	2197	2531	513.4	7.974	3.65
3C	15	26.314	40.625	195	2208	2528	537.6	7.957	3.50
3C	30	25.756	40.667	176	2150	2528	410.2	8.053	4.06
4C	1.8	26.819	40.565	202	2150	2530	424.0	8.040	4.10
4C	12.4	26.686	40.557	198	2154	2533	424.4	8.040	4.09
4C	36.9	26.669	40.557	190	2152				
5C	1.7	26.845	40.604	193	2213	2533	547.9	7.951	3.52
5C	15	26.822	40.602	191	2214	2530	558.8	7.943	3.47
5C	30.2	26.791	40.594	185	2148				
5C	51	26.796	40.595	184	2149	2535	415.1	8.048	4.17
6C	1.6	26.770	40.479	187	2230	2536	581.3	7.931	3.39
6C	18.3	26.773	40.478	188	2161	2540	427.3	8.039	4.11
6C	33.5	26.821	40.520	183	2224	2538	565.5	7.941	3.46
6C	53.3	26.843	40.531	181	2223	2538	561.9	7.943	3.48
6B	1.4	26.212	40.295	191	2164	2601	348.3	8.119	4.72
6B	20.4	26.219	40.291	187	2167	2542	424.6	8.043	4.06
6B	40	26.217	40.292	184	2233	2539	568.2	7.941	3.39
6B	57.5	26.218	40.290	182	2164	2543	418.5	8.048	4.10
6B	1.4	26.212	40.295	191	2232	2538	568.9	7.940	3.38
6B	57.5	26.218	40.290	182	2235	2540	571.9	7.938	3.37
Mean					2174	2526	476	8.004	3.79
Std. Dev					46.96	37.77	79.17	0.058	0.38
Data from May 2019									
Station	Depth	Temperature	Salinity	O2	DIC	TA	pCO2	pHcalc	Ω Ar
	m	°C		μmol kg^{-1}	μmol kg^{-1}	μmol kg^{-1}	μatm		
1C	1.7	27.043	41.026	190	2198	2556	483.7	7.996	3.89
1C	10	26.730	40.999	186	2197	2557	475.2	8.003	3.90
2C	1.6	27.599	40.757	207	2163	2552	431.8	8.035	4.21
2C	21.8	25.138	41.128	177	2206	2548	479.9	8.000	3.68
3C	1.7	27.527	40.451	211	2155	2546	422.0	8.043	4.24
3C	15.3	24.380	40.862	202	2214	2563	454.7	8.023	3.76
3C	29.6	24.505	41.201	166	2222	2555	490.9	7.994	3.58
4C	1.8	27.320	39.597	199	2134	2528	397.2	8.065	4.31
4C	15.8	23.387	40.310	229	2188	2548	406.7	8.063	3.86
4C	37	23.797	40.747	177	2215	2547	471.0	8.010	3.58
5C	1.6	27.124	39.274	161	2138	2513	417.3	8.047	4.12
5C	15.8	23.601	39.870	169	2171	2535	394.5	8.073	3.91
5C	32.6	22.600	40.190	138	2200	2535	432.4	8.041	3.60
5C	50.6	22.185	40.275	128	2203	2543	420.7	8.052	3.64
6C	1.8	27.263	39.304	131	2143	2505	440.4	8.027	3.98
6C	14.4	25.015	39.640	146	2169	2518	434.9	8.036	3.80
6C	33.3	21.252	40.075	143	2218	2538	437.4	8.039	3.44
6C	58.5	21.421	40.593	115	2214	2546	426.9	8.047	3.54
6B	1.7	27.297	39.361	185	2146	2509	441.5	8.027	3.99
6B	18.2	23.136	39.889	181	2152	2526	369.7	8.095	3.99
6B	34.4	21.400	40.032	137	2222	2535	453.4	8.026	3.37
6B	58.5	20.794	40.624	119	2227	2545	443.5	8.034	3.39
6B	1.7	27.297	39.361		2142	2474	489.2	7.986	3.66
6B	58.5	20.794	40.624		2227	2551	434.0	8.043	3.45
Mean					2186	2536	440	8.034	3.79
Std. Dev					32.31	20.52	31.37	0.027	0.27

Table 2
Comparison of the average concentrations for carbonate system parameters and salinity in all samples with the average concentrations in only surface samples (<2 m),

	DIC	TA	pCO_2	pH_{calc}	Ω_{Ar}	S_p
Grand Average (All Data)	2180	2532	457	8.02	3.79	40.41
Std. Dev.	40	30	61	0.05	0.32	0.48
Grand Average (Surface Data)	2171	2528	458	8.01	3.78	40.36
Std. Dev.	40	35	62	0.05	0.33	0.55

column was mostly well mixed.

In December 2018, temperature ranged from 26.2° to 26.8 °C and salinity (S_p) ranged from 40.3 to 42.0. There was more variability in May 2019 when temperatures ranged from 20.8° to 27.6 °C and salinity (S_p) ranged from 39.3 to 42.2. The water column was homogeneous for all hydrographic and chemical properties in December 2018 due to winter mixing, but in May 2019 a thermocline had developed. Similar summer stratifications were reported previously. The Chl-a concentrations for both seasons (not shown) were uniform throughout the water column and ranged from 0.65 to 2.07 μg kg^{-1}. There were no significant differences along our sampling section. Nevertheless, at offshore Station 6B, in May 2019, O_2 decreased by 66 μmol kg^{-1} from the surface (185

μmol kg^{-1}) to the bottom water (119 μmol kg^{-1}). Hypoxia (defined by $[O_2] < 62$ μM) in the bottom water of the deepest stations did not occur at the time of our sampling, but has been previously observed in late summer.

In December 2018, there was no systematic variation with depth for DIC or TA, as DIC ranged from 2065 to 2235 μmol kg^{-1}, and TA ranged from 2415 to 2601 μmol kg^{-1}. The total variabilities for DIC and TA were 47 μmol kg^{-1} and 38 μmol kg^{-1}, respectively. These are about a factor of 10 larger than our stated analytical precision. Part of this is due to slightly lower values of DIC and TA at stations 1C and 2C, the two stations closest to shore. In May 2019, the total variability was larger and DIC ranged from 2134 to 2227 μmol kg^{-1}, while TA ranged from 2505 to 2556 μmol kg^{-1}. The larger variability was due to the increase in DIC and TA, by as much as 85 μmol kg^{-1} (+3.9%) for DIC and 77 μmol kg^{-1} (+3.1%) for TA, from the surface to the bottom at the deepest, offshore stations 5C and 6B, 6C. These increases reflect respiration, as seen by the decrease in O_2, and dissolution of $CaCO_3$ in the bottom waters.

pCO_2, pH, $[CO_3^{2-}]$ and $\Omega_{aragonite}$ were calculated from DIC and TA. The pH_{calc} calculated from DIC and TA (total H^+ ion scale) ranged between 7.93 and 8.12. Calculated pCO_2 ranged from 348 to 581 μatm, with no clear increase with depth. The average pCO_2 in surface seawater was 460 ± 60 μatm. The water column was supersaturated at all depths with respect to calcite ($\Omega_{calcite}$ = 4.97 to 6.95) and aragonite ($\Omega_{aragonite}$ = 3.37 to 4.72).

4. Discussion

Changes occur in the carbonate system chemistry of surface seawater in the Arabian Gulf after it enters from the Arabian Sea (Gulf of Oman) through the Strait of Hormuz (Brewer and Dyrssen, 1985). Unfortunately, our samples are limited to the Exclusive Economic Zone (EEZ) of Qatar (Fig. 1). To enable analysis on a larger spatial scale, we have included a comparison of our 2018/2019 data with the 1977 data from Brewer and Dyrssen (1985), which covered the entire Gulf. This introduces some uncertainty because the Brewer and Dyrssen data were obtained 44 years ago (before Certified Reference Materials (CRMs) were available) and provides only one time point for the surface source water to the Gulf from the Strait of Hormuz. The source water flowing through Hormuz reflects upwelling of seawater, with high DIC and CO_2, from the oxygen minimum zone in the Gulf of Oman and the Arabian Sea, that occurs as shallow as 110 m (Brewer and Dyrssen, 1985). That upwelling is likely variable and once at the surface there may be additional outgassing of CO_2 or an increase in DIC due to mixing with seawater containing anthropogenic CO_2.

4.1. pCO_2 in surface seawater

The pCO_2 in surface seawater of the Qatari EEZ in the central Gulf was higher than atmospheric pCO_2, which was 412 ppm in 2018. The grand average for all surface data was pCO_2 = 458 ± 62 μatm but the average value of 476 ± 79 μatm in December 2018 was significantly higher than the value of 440 ± 31 μatm in May 2019. Hence, the Gulf is a source of CO_2 to the atmosphere. Even though the surface seawater is supersaturated with respect to the atmosphere, ocean acidification is still occurring because, as atmospheric CO_2 increases, the outgassing of CO_2 from the surface of the Gulf will wane and more CO_2 will remain in the Gulf, as it becomes more acidic.

If atmospheric CO2 continues to increase at its present rate (2.4 ppm y^{-1}), and seawater pCO_2 stays the same, the air-sea gradient would reverse in approximately 2038. This extrapolation may not be realistic because of the tendency for surface seawater to track the increase in atmospheric CO_2 and not remain constant (Takahashi et al., 2014). If that condition applies, pCO_2 in surface seawater should maintain its degree of supersaturation and remain a source of CO_2 to the atmosphere farther into the future. However, if TA and DIC entering the Gulf are controlled mostly by upwelling in the Arabian Sea, surface pCO_2 may not closely track atmosphere CO_2.

Another approach is to use the metric ($\Omega_{aragonite}$) to evaluate the impact of OA on corals. Orr et al. (2005) suggested that corals are adversely impacted when values for $\Omega_{aragonite}$ decrease to around 3. Most of our present values for $\Omega_{aragonite}$ in surface seawater are around 3.5 to 4.0 (Table 1). Assuming average surface values of S = 40.3, T = 26.05 °C and TA = 2528 μmol kg^{-1}, we calculate that $\Omega_{aragonite}$ will reach values of 3 when pCO_2 reaches about 665 μatm. At the present rate of increase of atmospheric CO_2 of 2.4 ppm y^{-1}, this will not occur until about 2125.

pCO_2 in seawater is controlled by the TA to DIC ratio, as well as temperature and salinity. The elevated levels of pCO_2 we observed in the Gulf reflects a balance between the following processes.

a. As temperature and salinity increase, DIC and TA also increase, but in addition the carbonate system equilibrium constants change, resulting in increases of pCO_2.
b. Some CO_2 can be lost by gas exchange, thus decreasing DIC and pCO_2.
c. The impact of biological production varies depending on the process: net primary production (ΔCH_2O) will consume CO_2 whereas CO_2 is produced during net calcification ($\Delta CaCO_3$).

4.2. Variability of pCO_2 by increasing T and S

Surface seawater enters the Gulf through the Strait of Hormuz. Taking values of T (22.16 °C), S (36.6), TA (2380 μmol kg^{-1}) and DIC (2075 μmol kg^{-1}) for the Strait of Hormuz from Brewer and Dyrssen (1985), pCO_2 would be 388 μatm. Temperature (ΔT = 22.16° to 26.8°) and salinity (ΔS = 36.6 to 40.0) increase in surface seawater after entering the Gulf. The carbonate system acidity constants (K_1', K_2' and K_H') also change, as they are a function of T and S. We carried out hypothetical model calculations to estimate how much pCO_2 would increase due to increases in T and S alone, in the absence of biogeochemical processes (Table 3). While keeping TA and DIC constant at the initial values in the Strait, we calculated that the increase of T alone, from 22.16 °C to 26.8 °C, would increase pCO_2 to 493 μatm. Evaluating the impact of increasing S to 40.0 is more complicated because TA and DIC change with S. Increasing S from 36.6 to 40.0 increases TA to 2604 μmol kg^{-1} and DIC to 2270 μmol kg^{-1} (slightly higher than observed). As a result of this change in S alone we calculate that pCO_2 would increase to 447 μatm. As a result of the increase in both

Table 3
pCO_2 varies with S and T. We assumed values for TA (μmol kg^{-1}) and DIC (μmol kg^{-1}) in surface seawater entering through the Strait of Hormuz with initial values of S = 36.6 and T = 22.16. We calculated how pCO_2 varies individually for S increasing to 40.0 and T to 26.8 and then both T and S increasing. Then we calculated the individual changes due to loss of CO_2 by gas exchange, calcification and net primary production. The carbonate system equilibrium constants are from Millero (2010).

	S	T	TA	DIC	pCO_2
		°C	μmol kg^{-1}	μmol kg^{-1}	μatm
Hormuz	36.6	22.16	2380	2075	389
ΔT alone	36.6	26.8	2380	2075	493
ΔS alone	40.0	22.16	2604	2270	447
ΔT + ΔS	40.0	26.8	2604	2270	537
ΔT + ΔS – gas exchange	40.0	26.8	2604	2235	464
ΔT + ΔS + calcification	40.0	26.8	2474	2180	577
ΔT + ΔS -net primary production	40.0	26.8	2604	2119	295
ΔT + ΔS -gas exchange +calcification -net primary production	40.0	26.8	2474	2128	458

T and S, pCO_2 would increase to 537 μatm, more than enough to explain the high pCO_2 observed (458 ± 62 μatm).

The average pCO_2 we observed in surface seawater of the Gulf, was less than predicted by this hypothetical calculation considering increases of T and S alone. The lower pCO_2 we observed could be due to changes in DIC and TA because of loss of CO_2 by gas exchange or net biological production.

4.3. Air-Sea Flux of CO_2

CO_2 is lost from surface seawater of the Gulf by gas exchange. We calculated the flux of CO_2 across the air – sea interface using the stagnant boundary layer model (e.g., Liss and Slater, 1974):

$$Flux_{CO2} = k \cdot K_H' \left(pCO_{2sw} - pCO_{2atm}\right) = K\,\Delta pCO_2 \quad (4)$$

where k is the piston velocity (a function of wind speed), K_H' is the solubility of CO_2 in seawater (a function of T and S_p), K equals k · K_H', and ΔpCO_2 is the gradient of CO_2 across the air-sea interface.

The predominant winds are northwesterlies throughout the year with weaker winds in September and stronger winds in February. The stronger shamal winds occur occasionally in both summer (June) and winter (February). Windspeed data for the EEZ of Qatar are available from Aboobacker et al. (2021) who utilized winds from the ERA5 reanalysis product of the European Centre for Medium-range Weather Forecasts (ECMWF). Measured winds (at 10 m height) at Doha Airport were used to validate the ERA5 winds. The relevant winds for this study were offshore from Doha where mean winds were 5.1 ± 2.5 m s^{-1}. The mean wind speed corresponds to a piston velocity of k = 6.2 cm h^{-1} or 1.6 m d^{-1} (Wanninkhof, 1992). Even though the piston velocity varies with wind speed, using an average value is sufficient for this study because of the small magnitude and low variability in wind speed and the large variability in estimates of piston velocity as a function of wind speed (e.g., Wanninkhof and McGillis, 1999).

The solubility (K_H') of CO_2 at $T = 25$ °C and $S_p = 40$ is 20×10^{-3} mol kg^{-1} atm^{-1}. The average pCO_2 in surface seawater in the Gulf was 476 μatm in December 2018 and 440 μatm in May 2019. Whereas regional differences may exist, we assumed that local atmospheric pCO_2 equaled values measured at Moana Loa of 412 μatm in both December 2018 and June 2019 (from Moana Loa running means at https://gml.noaa.gov/ccgg/trends/). Therefore, ΔpCO_2 was 66 ± 25 μatm in Dec 2018 and 28.5 ± 15 μatm in May 2019. The resulting fluxes of CO_2 to the atmosphere were 2.1 ± 0.5 mmol C m^{-2} day^{-1} or 0.8 mol C m^{-2} y^{-1} in December 2018 and 1.0 ± 0.4 mmol C m^{-2} day^{-1} or 0.4 mol C m^{-2} y^{-1} in May 2019.

Comparison of these air-sea CO_2 fluxes with fluxes over healthy coral reef systems elsewhere, provide a reference for what fluxes might be if corals or other forms of calcification in the Qatari EEZ are producing $CaCO_3$ and CO_2. For example, the net annual area-specific flux of CO_2 to the atmosphere in Kaneohe Bay, Hawaii was 1.45 mol C m^{-2} y^{-1} (Fagan and Mackenzie, 2007) and averaged 1.24 ± 0.33 mol C m^{-2} y^{-1} over a nine-year data set (Terlouw et al., 2019). Lonborg et al. (2019) calculated an average air-sea flux of CO_2 to the atmosphere over the Great Barrier Reef of 0.52 mol C m^{-2} y^{-1}. Though pCO_2 in seawater over growing corals varies on diurnal and seasonal time scales, on average it is greater than atmospheric pCO_2 and the fluxes calculated for the Qatari EEZ are about 25% to 50% of values seen for healthy coral systems.

The consequence of gas exchange is to reduce DIC. If DIC decreases and TA stays constant, pCO_2 decreases. We used the CO_2 flux, a water residence time of 1 yr and an average depth of 35 m, to estimate how much DIC was decreased by CO_2 outgassing. Gas exchange appears to decrease DIC by about 35 μmol kg^{-1}. This loss of DIC was added to the model calculations that included increases in T and S (Table 3). As a consequence of CO_2 loss by gas exchange, pCO_2 would be reduced to 464 μatm, similar to that observed.

4.4. Net biological production

Net biological production (of CH_2O or $CaCO_3$) produces changes in TA and DIC that also influence pCO_2. After entering the Gulf, both TA and DIC in surface seawater increase due to evaporation as salinity increases from 36.5 to 41 (Fig. 2a, b). One way to examine possible temporal changes is by comparing the distributions of TA and DIC versus S in the 2018/2019 data set with that of 1977. The data from 2018/2019 and 1977 generally agree well except for a few data points in Dec 2018 at stations 1C and 2C, close to the coast of Qatar, which had higher S and lower TA and DIC. These data points are circled in Fig. 2a and b. These low values may be due to enhanced primary production and net calcification near shore. The salinity was also slightly higher at these stations and effluent from desalination plants may be a possible source, but it is unknown how that would result in lower TA and DIC. There is also one anomalously high data surface point for TA and DIC at station 6B, that does fall on the same DIC vs S and TA vs S trend as the Brewer and Dyrssen (1985) data. In the 1977 data there were a few stations at the far north, near Kuwait and Iraq, with lower salinity, TA and DIC due to riverine input. The riverine influence is only important in the northern part of the Gulf and does not extend as far south as the Qatari EEZ (Anderson and Dyrssen, 1994).

It is possible that over the 51-year period between samplings, as atmospheric CO_2 increased from 334 to 412 ppm, DIC concentrations could have increased appreciably, as much as ~50 μmol kg^{-1} at given TA, temperature and salinity. It is probably safe to say that S has remained constant over those decades. An increase in DIC of 50 μmol kg^{-1}, due to the increase in atmospheric CO_2, should result in an offset in a plot of DIC versus S, but the DIC and TA versus S data (Figs. 2a, b) suggests that both TA and DIC, for a given salinity, have remained reasonably constant over the 51-year interval between samplings. This supports our argument that DIC and salinity in source water entering Hormuz are controlled by upwelling of subsurface, suboxic seawater in the Arabian Sea, with lower O_2 and higher DIC. Realizing the limitations of our data set, we use the 1977 data for the surface seawater in the Strait of Hormuz as the best approximation available for the surface input to the Arabian Gulf.

The relationship between TA and DIC in surface seawater of the Qatari EEZ is shown in Fig. 3. There was no statistical difference between the average values of TA and DIC in the surface Gulf water for the 2018 and 2019 sampling periods, but we identify them separately in the figure. Also shown are the surface water data and the concentrations in the inflowing surface water at the Strait of Hormuz from 1977 (Brewer and Dyrssen, 1985). In the 1977 data, TA increased more than DIC and the slope (ΔTA/ΔDIC) was 1.23 ± 0.04. The regression for the 1977 data had high significance ($R^2 = 0.95$). Even though the DIC versus S plots showed little difference between 1977 and 2018/2019 (Figs. 2a,b), the slope for the 2018/2019 data was 0.29 ± 0.12 suggesting that the change in DIC was larger than TA. However, the significance of that regression was poor ($R^2 = 0.27$), possibly because the data covered a smaller concentration range. A t-test of the two slopes gives a t value of 11.1 and a p value of 10^{-17}. As p is much <0.05, the slopes of these regressions are significantly different.

To separate the effect of biogeochemistry on the carbonate system from the changes due to evaporation we normalized individual surface TA and DIC concentrations to a constant salinity (S = 40), using:

$$NTA\ (or\ NDIC) = \frac{TA\ (or\ DIC)*40}{S} \quad (5)$$

Normalized values of NTA are plotted versus NDIC in Fig. 4. We also show the surface water concentrations from the Strait of Hormuz and the surface data for the entire Gulf from 1977. NTA and NDIC decrease as surface seawater flows to the north, after entering through Hormuz. The slope for the 1977 data was >1 (1.06 ± 0.03) and more significant (R^2 = 0.96), possibly because the data cover a larger spatial and concentration range. The combined data sets from 2018/2019 decrease with a slope of

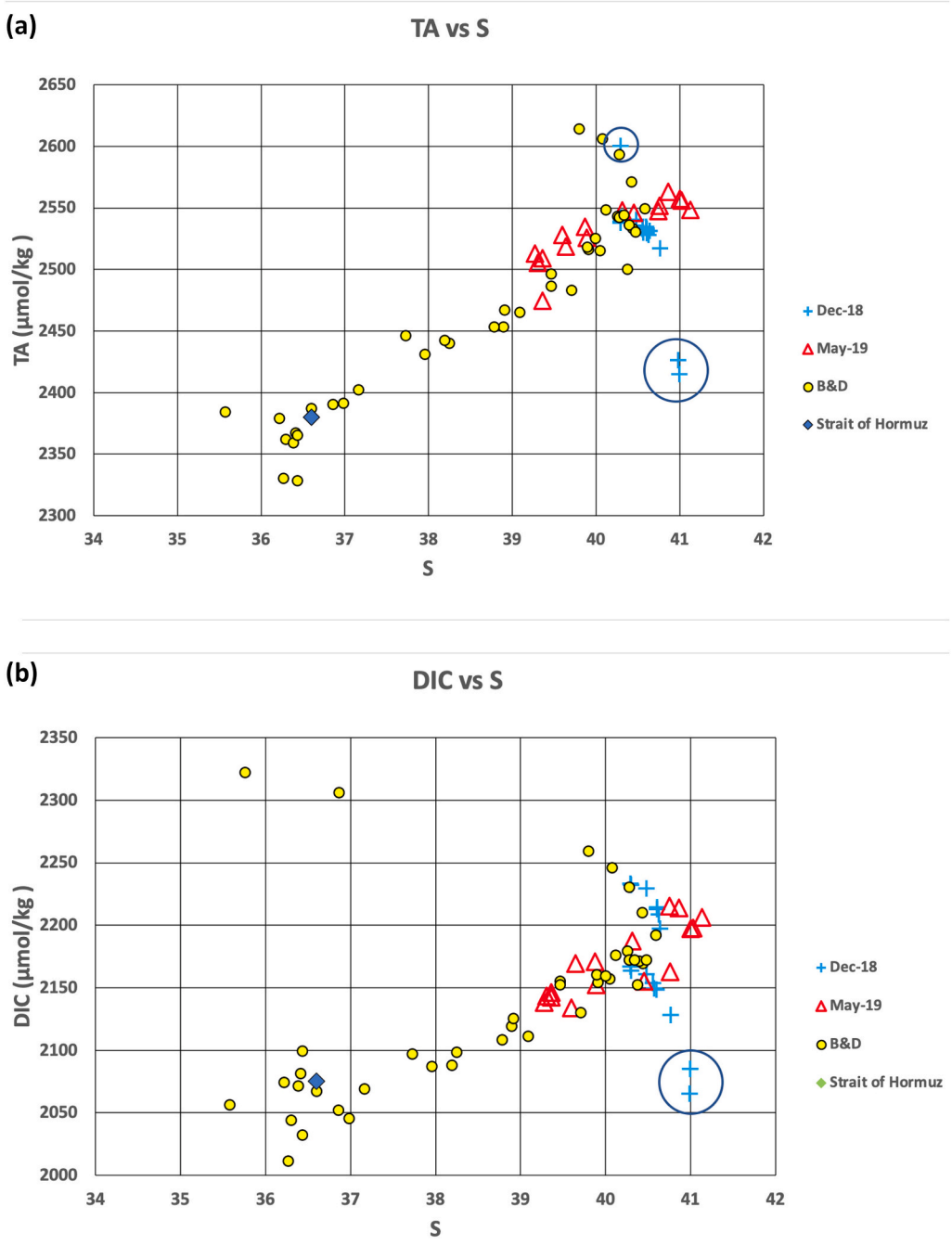

Fig. 2. Comparison of the 2018/2019 data with that from 1977.
a) TA versus S; b) DIC versus S.

$\Delta NTA/\Delta NDIC = 0.35 \pm 0.12$ with $R^2 = 0.20$. The three data points mentioned previously from stations 1C, 2C and 6B, that don't fall on the main trend of the data, were not included. A t-test confirmed that the slopes of these regressions are significantly different ($t = 7.2$ and $p = 10^{-10}$).

The traditional approach to interpret the slope of ΔNTA/ΔNDIC uses a model that describes the formation of organic matter (CH_2O) and calcium carbonate ($CaCO_3$) with simple stoichiometries. The carbon removed, and changes in DIC and TA, due to $CaCO_3$ formation and CH_2O production can be predicted using the equations below (Broecker and Peng, 1982).

$$Ca^{2+} + CO_3^{2-} = CaCO_3 \ \Delta DIC = -1 \ \Delta TA = -2 \quad (6)$$

$$CO_2 + H_2O = CH_2O + O_2 \ \Delta DIC = -1 \ \Delta TA = 0 \quad (7)$$

Both reduce DIC but only $CaCO_3$ formation reduces TA. This simple model ignores the impact of acid produced by oxidation of NH_4^+ to NO_3^- and acid consumed by conversion of NO_3^- to organic amines (Brewer and Goldman, 1976). This NO_3^- effect can be neglected in the Gulf because NO_3^- concentrations are so low.

If we assume that the Strait of Hormuz data from Brewer and Dyrssen (1985) approximates the source water, the observed changes in NTA and NDIC for the 2018/2019 data (slope = 0.35) are consistent with a ratio of carbon removal by $CaCO_3$ formation to carbon uptake by net photosynthesis ($\Delta CaCO_3 / \Delta OrgC$) of ~0.21 (or 1:2.86). For the 1977 data, the slope of 1.06 corresponded to $\Delta CaCO_3 / \Delta OrgC$ of 2.5 (or 2.5:1). The slope was ~12 times larger in 1977 than in 2018/2019. The

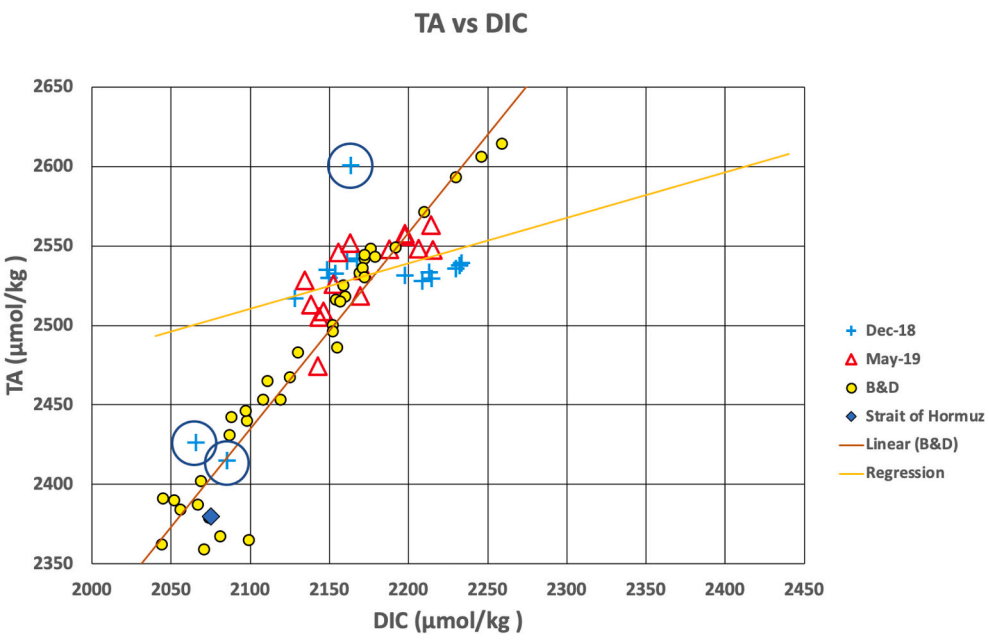

Fig. 3. Alk versus DIC in surface seawater of the Exclusive Economic Zone (EEZ) of Qatar in the Arabian Gulf. The units for Alk and DIC are µmol kg^{-1}. The data point for 1977 from the Strait of Hormuz is from Brewer and Dyrssen (1985). Separate linear regressions are given for the 1977 data (B&D) and the 2018/2019 data.
The regression for the 1977 data is Y = 1.23 ± 0.04 X – 153 ± 91 (R^2 = 0.95).
The regression for the 2018/2019 data is Y = 0.29 ± 0.12 X + 1910 ± 255 (R^2 = 0.27).

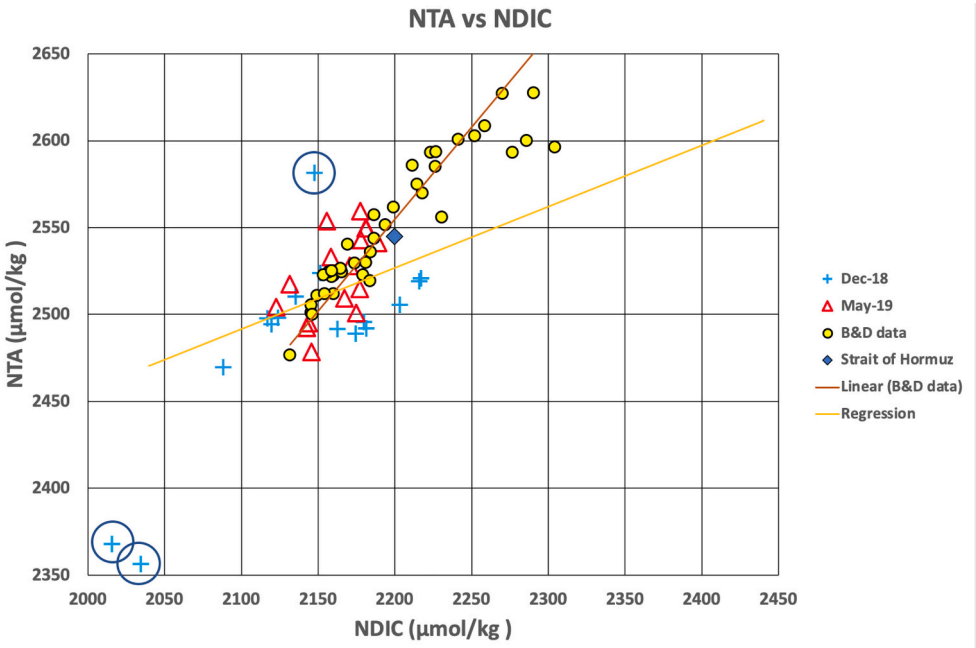

Fig. 4. NTA versus NDIC in surface seawater of the Qatari EEZ of the Arabian Gulf in December 2018 and May 2019. Surface data from 1977 for the entire Arabian Gulf and Strait of Hormuz from Brewer and Dyrssen (1985) are shown for comparison. The regression for the 1977 data is Y = 1.06 ± 0.03 X + 216 ± 74 (R^2 = 0.96). The regression for the 2018/2019 data is Y = 0.35 ± 0.12 X + 1752 ± 91 (R^2 = 0.20).

distributions of NTA and NDIC in the Gulf indicate that $CaCO_3$ formation is a major process and that, because the slopes of NTA/NDIC are significantly different, $CaCO_3$ formation was more important in 1977 than in 2018/2019. For comparison, the average ratio for carbon removal from the euphotic zone of average open ocean surface seawater, using this same model, is about 0.05 (or 1:18) (Emerson and Hedges, 2012). Therefore, even though carbon removal by $CaCO_3$ formation, relative to net photosynthesis, has been reduced since 1977, it is still about 4 times larger than in the average open ocean.

This model neglects a decrease in DIC due to loss of CO_2 to the atmosphere by gas exchange. Loss of CO_2 by gas exchange has the same impact on the ΔNTA/ΔNDIC ratio as production of CH_2O (Eq. 7). The characteristic residence time for gas exchange of CO_2 is less than one year for this shallow, well-mixed water column (Williams and Follows, 2011). The residence time for the whole Arabian Gulf is about 1.3 years (Sheppard et al., 2010) and the residence time for the Qatari EEZ must be much less than that. The residence times are short enough that loss of CO_2 by gas exchange will be reflected by changes in DIC concentrations. We conclude that the decrease in DIC (ΔNDIC), and the resulting ratio of ΔNTA/ΔNDIC, are due to both a loss of CO_2 by gas exchange (F_{CO2}) as well as CH_2O formation. Our challenge is to determine the relative importance of these two processes.

The NTA / NDIC (slope = 0.35) in the Arabian Gulf, and the corresponding $\Delta CaCO_3$ / (ΔOrgC or F_{CO2}) removal ratios (1:2.86), can be

compared to those measured in other coral reef systems in the Middle East. In the eastern central Red Sea, at Al-Fahal reef, the slope of the regression between NTA and NDIC was 0.42 (Saderne et al., 2019). That slope closely corresponds to the global mean for coral reefs of 0.41 ± 0.18 (Cyronak et al., 2018).

4.5. Net formation of $CaCO_3$

Our ΔNTA/ΔNDIC data suggest that $CaCO_3$ is forming, and this should be a source of CO_2. Unfortunately, there have been few studies of calcification in the water column or sediments of the Qatari EEZ. Quigg et al. (2013) found that of 125 plankton species identified, 66% were diatoms, 33% were dinoflagellates and the remaining 1% cyanobacteria (mostly filamentous *Trichodesmium thiebautii*). No carbonate-secreting pelagic micro-organisms, such as coccolithophores or planktonic foraminifera, were identified. Similar results were reported by Polikarpov et al. (2016). Whiting events, periods of high levels of suspended fine-grained $CaCO_3$ particles in the water, have been identified in the Gulf using Aqua/Terra MODIS images, but are thought to be due to sediment resuspension associated with high winds that lasted for several days (Shanableh et al., 2021). Such events have not been directly sampled to identify whether the $CaCO_3$ is calcite or aragonite. Whereas calcifying phytoplankton appear to be absent from the water column, highly diversified benthic foraminiferal communities have been observed (Amaoa et al., 2019). As there are no carbonate-secreting organisms in the water column, we must assume that calcification is by corals or in the sediments.

Historically, coral communities around Qatar were among the most widespread in the region and were a valuable economic resource (Rezai et al., 2004; Burt et al., 2015). These coral communities were dominated by *Acropora* (staghorn) table corals to water depths of 4-5 m and massive *Porites* corals from 5 m to 10 m depth. Unfortunately, there has been a general decline in the ecological health of these corals due to recent bleaching events caused by extreme ocean warming. Significant events occurred in 1996, 1998, 2002 and 2017 when sea surface temperature (SST) sometimes reached >37 °C (Grizzle et al., 2016; Burt et al., 2019). These events resulted in near total loss of coral from shallow (<3 m) habitats around Qatar. The damage due to bleaching was exacerbated by anthropogenic activities - sedimentation from dredging and pollution from the growing urban and industrial sectors (Burt, 2014). Off-shore coral assemblages were also impacted by the bleaching events and most (e.g., the regions near Fuwaurit and Al-Ashat) are now covered by bare rock, sand, algal turfs and dead coral rubble (Al-Ghadban et al., 1998; Sheppard et al., 2010; Billeaud et al., 2014; Burt et al., 2015; Hassan et al., 2018). Nevertheless, a few isolated, healthy sites still exist, like Umm Al-Arshan (Burt et al., 2015) and Halul Island (Abdel-Moati, 2006).

Though corals in the Arabian Gulf are not thriving, studies here and elsewhere suggest that calcification may still be occurring (Howells et al., 2016; Claar et al., 2020; Romanó de Orte et al., 2021; Courtney et al., 2022; Radice et al., 2022). The presence of some corals in thermally stressed environments suggests that some populations can cope with elevated temperatures (Craig et al., 2001; Smith et al., 2022). Some southern Gulf corals are associated with a stress-tolerant algal symbiont, *Cladocopium thermophilum* (Howells et al., 2020) indicating thermal tolerance. Even when there is extensive mortality in coral assemblages, recolonization may occur within a few years (Burt et al., 2015). Nevertheless, the overall coral cover remains depressed (Foster et al., 2013) and the assemblage transitioned from *Acropora* to more hardy stony corals such as *merulinids*, *poritids*, *siderastreids*, and *dendrophyllids* ((Mohammed and Al-Ssadh, 1996).

The precipitation of $CaCO_3$ is promoted by the elevated saturation states of the waters of the Gulf with respect to calcite ($\Omega_{calcite}$ = 5.0 to 7.0) and aragonite ($\Omega_{aragonite}$ = 3.4 to 4.7). The calcification reaction can be described as consuming two moles of bicarbonate and forming one mol of $CaCO_3$ and one mole of CO_2 (Eq. 8), and is therefore a source of CO_2,

$$2\,HCO_3^- + Ca^{2+} = CaCO_3\downarrow + CO_2\uparrow + H_2O \quad (8)$$

During calcification, seawater becomes more acidic due to the removal of carbonate and bicarbonate ions, and the resulting decrease in pH increases the abundance of dissolved CO_2 (Stumm and Morgan, 1995). pCO_2 increases and, in an open system, the CO_2 produced is either taken up for primary production or escapes to the atmosphere. This simplistic representation of the calcification process suggests that for each mole of $CaCO_3$ deposited, one mole of CO_2 is liberated. The relationship is close to 1:1 in freshwater, but is reduced in buffered seawater where only ≈ 0.62 mol of CO_2 is liberated per mole of $CaCO_3$ deposited (Ware et al., 1991; Smith and Gattuso, 2011).

We can quantify net $CaCO_3$ formation with the tracer Alk* (Carter et al., 2014). Regions with net carbonate precipitation are characterized by negative Alk*. Whereas the absolute magnitude of this tracer in a shallow coastal environment, like the Gulf, may be uncertain because of sediment interactions and riverine inputs, its trends are probably valid. Calculation of Alk* requires the concentration of NO_3^- (Eq. 1). We did not have NO_3^- data for our sample set, but three previous studies in different seasons have found surface concentrations of NO_3^- to be consistently ≤0.5 μmol kg^{-1} (Quigg et al., 2013. Accordingly, we assumed surface NO_3^- concentrations of 0.5 μmol kg^{-1} for these calculations. All values of Alk* calculated from our surface seawater data were negative and ranged from −50 to −240 μmol kg^{-1}. This supports the finding in the previous section that the NTA / NDIC ratios reflect substantial $CaCO_3$ formation in the Gulf. Alk* values of −247 μmol kg^{-1} and -240 μmol kg^{-1} were previously calculated, using the same model, for the Red Sea and the Trucial Coast region of the Arabian Gulf, respectively (Carter et al., 2014).

In order to examine the spatial trends of $CaCO_3$ precipitation in the Gulf, we calculated ΔAlk*, the difference between specific locations in the Qatari EEZ and the surface water entering through the Strait of Hormuz. The surface seawater entering through the Strait already has a negative Alk* of −44 μmol kg^{-1}. ΔAlk* decreased with increasing distance northward from Hormuz to values as large as −310 μmol kg^{-1} (Fig. 5). The average decrease of Alk* was −130 μmol kg^{-1} (about the same decrease in NTA seen in Fig. 4), which corresponds to a calcification of 65 μmol C kg^{-1}. According to the "0.6 rule", this would result in the addition of 40 μmol CO_2 kg^{-1} and a decrease of TA by 130 μmol kg^{-1}. For a closed system, DIC would be reduced by the HCO_3^- consumed (−130 μmol kg^{-1}), corrected for the CO_2 produced (+0.6 × 65 = 40 μmol C kg^{-1}), or − 90 μmol C kg^{-1}. These decreases in TA and DIC were added to the model calculations that accounted for increases in T and S (Table 3). As a result, calcification would increase pCO_2 by 40 μatm to 577 μatm, much higher than the observed value (458 μatm).

4.6. Net autotrophic production

Net autotrophic production decreases DIC, at nearly constant TA, and lowers pCO_2. Unfortunately, there have been few studies of this process in the Qatari EEZ.

The surface waters of the Gulf, especially in the Qatari EEZ, are oligotrophic. The euphotic zone (<35 m) usually extends to the seafloor. The surface waters are characterized by low concentrations of nitrate (<0.5 μmol kg^{-1}), biomass (0.65–2.07 μg Chl a kg^{-1}) and low rates of primary productivity (5.8 to 40.3 μg C kg^{-1} h^{-1}) (Quigg et al., 2013). Spike experiments by Quigg et al. (2013) showed that this nutrient-stressed ecosystem was nitrogen limited.

According to our data, the slope of ΔNTA versus ΔNDIC yielded a $\Delta CaCO_3/(\Delta OrgC$ or $F_{CO2}) = 1{:}2.86$ (Fig. 4) and thus the DIC removed to form organic carbon or lost by gas exchange is larger than that removed to form $CaCO_3$. For example: for each 10 μmol DIC removed as organic carbon or lost by gas exchange, 3.5 will be removed as $CaCO_3$. Accordingly, the decrease in TA will be 7 μmol. Because TA decreases

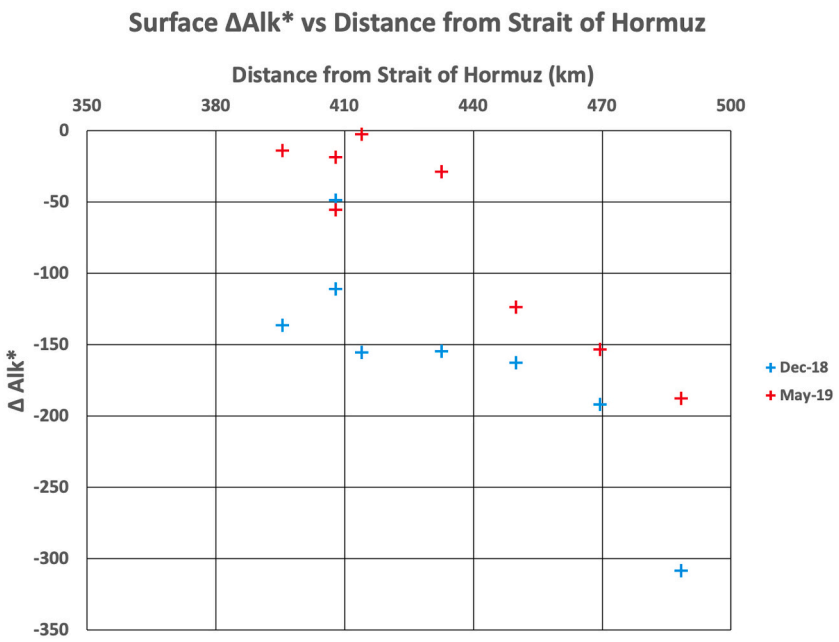

Fig. 5. ΔAlk* in the Qatari EEZ, calculated as the difference between the value of Alk* at individual stations and the value for the Strait of Hormuz. ΔAlk* is plotted versus distance from the Strait of Hormuz. The gradual decrease in ΔAlk* indicates progressive formation of $CaCO_3$.

more slowly than DIC, the pCO_2 goes down. Thus, surface water distributions of NDIC and NTA suggest that the net effect of biological processes in the Gulf is a net sink of CO_2. As net calcification increases pCO_2, to maintain pCO_2 invarient, net primary production must reduce pCO_2 by at least that amount.

Values of net community production that can be used to estimate the removal of DIC, are not available. Nonetheless, we can make a rough estimate using our data. Our average value of ΔAlk* (Fig. 5) suggests a net calcification of 65 μmol C kg^{-1}. Assuming $\Delta CaCO_3/\Delta OrgC = 1{:}2.86$, and $F_{CO2} = 0$, we calculate an upper limit for net formation of CH_2O of 186 μmol C kg^{-1}. As we previously estimated (Section 4.3), that F_{CO2} would decrease DIC by 35 μmol C kg^{-1}, the upper limit for DIC decrease by net primary production would be 151 μmol C kg^{-1}. If this decrease in DIC were added to the model calculations that account for increases in T and S (Table 3) pCO_2 would decrease to 295 μatm. This is much less than the observed value of 458 μatm.

We can ask the question in reverse. How much would DIC have to decrease, due to net primary production, to result in the observed pCO_2? A model calculation (Table 3) that accounts for increases in T and S, loss by gas exchange and changes due to calcification shows that DIC needs to be decreased to 2128 μmol kg^{-1} (−142 μmol kg^{-1}). Of this change, 90 μmol kg^{-1} is due to calcification and 35 μmol kg^{-1} is due to gas exchange. That leaves only 17 μmol C kg^{-1} as a lower limit for the DIC removed by net primary production. This is consistent with an oligotrophic food web dominated by remineralization rather than export. The discrepancy between 186 μmol kg^{-1} (estimated from ΔAlk*) and 142 μmol kg^{-1} is acceptable considering the large uncertainties in the different approaches. In the absence of better data, it appears that the role of biological production in the water column in controlling surface water pCO_2 cannot be definitively resolved, but appears to be negligible.

4.7. Conclusions: Controls on pCO_2

Our goal was to understand why the pCO_2 in surface seawater of the Arabian Gulf was greater than atmospheric values. Our approach was to use a hypothetical model where we assumed initial conditions for surface seawater entering the Gulf through the Strait of Hormuz and individually evaluated the importance of the different processes that control pCO_2 in surface seawater. The pCO_2 in the surface seawater of the EEZ of Qatar, in the Arabian Gulf, is controlled by the balance between sources and sinks of CO_2. We conclude that the largest source is due to the impact of increases in T and S on the carbonate system equilibrium constants with a smaller contribution due to net $CaCO_3$ formation. These sources are partly balanced by a sink due to CO_2 lost to the atmosphere by gas exchange and, probably minor, removal by net primary production. Future studies should strive to obtain basin scale data sets and resolve the relative uncertainties in these sources and sinks.

Author contributions

J.W.M. and O.Y. designed the research. Samples were collected by J. A-T, O.Y., E.A-A, P.V. and C.S. Hydrographic data were processed by C. S.. C.I. and J.W.M. wrote the manuscript. D.A. assisted with TA and DIC analyses. All authors edited the manuscript.

Declaration of Competing Interest

None of the authors have financial and personal competing interests to declare.

Data availability

The data used for preparing this study are available through BCO-DMO.

Murray, J. W., Yigiterhan, O. (2021) Hydrographic, nutrient, and carbonate system data from R/V Janan cruises in the Arabian Gulf in December 2018 and May 2019. Biological and Chemical Oceanography Data Management Office (BCO-DMO). (Version 1) Version Date 2021-12-29. http://lod.bco-dmo.org/id/dataset/833517

Acknowledgments

Alex Gagnon (UW) provided the analytical facility for alkalinity and dissolved inorganic carbon analyses. We utilized the financial support of Qatar Petroleum (QP) (Project Number QUEX-ESC-QP-TM-18/19) for the cruise preparation, sampling and shipping. Open Access funding provided by the Qatar National Library. Discussions with Katie Shamberger (Texas A&M), Alex Gagnon (UW), Julian Sachs (UW) and Isaiah

Bolden (UW), a review by Burke Hales (OSU) and editorial suggestions by Alfonso Mucci significantly improved the manuscript.

References

Abdel-Moati, M., 2006. Coral Reef Conservation in Qatar, Marine Conservation Forum. EWS-WWF, Abu Dhabi, UAE, pp. 1–34.

Aboobacker, V.M., Shanas, P.R., Veerasingam, S., Al-Ansari, E.M.A.S., Sadooni, F.N., Vethamony, P., 2021. Long-term assessment of onshore and offshore wind energy potentials of Qatar. Energies 14, 1178–1199.

Al-Ghadban, A.N., Abdali, F., Massoud, M.S., 1998. Sedimentation rate and bioturbation in the Arabian Gulf. Environ. Int. 24, 23–31.

Alosairi, Y., Imberger, J., Falconer, R.A., 2011. Mixing and flushing in the Persian Gulf (Arabian Gulf). J. Geophys. Res. 116, C03029. https://doi.org/10.1029/2010JC006769.

Amaoa, A.O., Qurbanb, M.A., Kaminski, M.A., Joydasc, T.V., Manikandanb, P.K., Frontalinid, F., 2019. A baseline investigation of benthic foraminifera in relation to marine sediments parameters in western parts of the Arabian Gulf. Mar. Pollut. Bull. 146, 751–766.

Anderson, L., Dyrssen, D., 1994. Alkalinity and total carbonate in the Arabian Sea. Carbonate depletion in the Red Sea and Persian Gulf. Mar. Chem. 47, 195–202.

Billeaud, I., Caline, B., Livas, B., Tessier, B., Davaud, E., Frebourg, G., Hasler, C.A., Laurier, D., Pabian-Goyheneche, C., 2014. The carbonate-evaporite lagoon of Al Dakhirah (Qatar): an example of a modern depositional model controlled by longshore transport. In: Martini, I.P., Wanless, H.R. (Eds.), Sedimentary Coastal Zones from High to Low Latitudes: Similarities and Differences, 388. Geological Society, London, pp. 561–587. Special Publications.

Bolden, I.W., Sachs, J.P., Gagnon, A.C., 2019. Temporally-variable productivity quotients on a coral atoll: Implications for estimates of reef metabolism. Mar. Chem. 217, 1–13.

Brewer, P.G., Dyrssen, D., 1985. Chemical oceanography of the Persian Gulf. Prog. Oceanogr. 14, 41–55.

Brewer, P.G., Goldman, J.C., 1976. Alkalinity changes generated by phytoplankton growth. Limnol. Oceanogr. 21, 108–117.

Broecker, W.S., Peng, T.-H., 1982. Tracers in the sea. Eldigio.

Burt, J., 2014. The environmental costs of coastal urbanization in the Arabian Gulf. In: City: Analysis of Urban Trends, Culture, Theory, Policy, Action, 18, pp. 760–770.

Burt, J.A., Smith, E.G., Warren, C., Dupont, J., 2015. An assessment of Qatar's coral communities in a regional context. Mar. Pollut. Bull. 105, 473–479.

Burt, J.A., Paparella, F., Al-Mansoori, N., Al-Mansoori, A., Al-Jailani, H., 2019. Causes and consequences of the 2017 coral bleaching event in the southern Persian/Arabian Gulf. Coral Reefs 1–23. https://doi.org/10.1007/s00338-00019-01767-y.

Carpenter, J.H., 1965. The Chesapeake Bay Institute technique for the Winkler dissolved oxygen method. Limnol. Oceanogr. 10, 141–143.

Carter, B.R., Toggweiler, J.R., Key, R.M., Sarmiento, J.L., 2014. Processes determining the marine alkalinity and calcium carbonate saturation state distributions. Biogeosciences 11, 7349–7362.

Claar, D.C., Starko, S., Tietjen, K.L., Epstein, H.E., Cunning, R., Cobbm, K.M., Baker, A.C., Gates, R.D., Baum, J.K., 2020. Dynamic symbioses reveal pathways to coral survival through prolonged heatwaves. Nat. Commun. https://doi.org/10.1038/s41467-020-19,169-y.

Courtney, T.A., Barkley, H.C., Chan, S., Couch, C.S., Kindinger, T.L., Oliver, T.A., Kriegman, D.J., Andersson, A.J., 2022. Rapid assessments of Pacific Ocean net coral reef carbonate budgets and net calcification following the 2014–2017 global coral bleaching event. Limnol. Oceanogr. https://doi.org/10.1002/lno.12159.

Craig, P., Birkeland, C., Belliveau, S., 2001. High temperatures tolerated by a diverse assemblage of shallow-water corals in American Samoa. Coral Reefs 20, 185–189.

Cyronak, T., Andersson, A.J., Langdon, C., Albright, R., Bates, N.R., Caldeira, K., et al., 2018. Taking the metabolic pulse of the world's coral reefs. PLoS One 13 (1), 1–17.

Dickson, A.G., 1990. Thermodynamics of the dissociation of boric acid in synthetic seawater from 273.15 to 318.15 K. Deep-Sea Res. 37, 755–766.

Dickson, A.G., Sabine, C.L., Christian, J.R., 2007. Guide to best practices for ocean CO2 measurements. PICES Special Publication 3.

Doney, S.C., Fabry, V.J., Feely, R.A., Kleypas, J.A., 2009. Ocean acidification: the other CO_2 problem. Annu. Rev. Mar. Sci. 1, 169–192.

Emerson, S., Hedges, J., 2012. Chemical Oceanography and the Marine Carbon Cycle. Cambridge University Press, 453pp.

Fagan, K.E., Mackenzie, F.T., 2007. Air-sea CO2 exchange in a subtropical estuarine-coral reef system, Kaneohe Bay, Oahu, Hawaii. Mar. Chem. 106, 174–191.

Foster, K.A., Foster, G., Al-Harthi, S., 2013. Coral assemblages in the southeastern Arabian Gulf (Qatar and Abu Dhabi, UAE): various stages of Acropora recovery a decade after recurrent elevated temperature anomalies. Open J Mar Sci 3, 28–39.

Grizzle, R.L., Ward, K.M., Al-Shihi, R.M.S., Burt, J.A., 2016. Current status of coral reefs in the United Arab Emirates: distribution, extent, and community structure with implications for management. Mar. Pollut. Bull. 105, 515–523.

Hassan, H.M., Castillo, A.B., Yigiterhan, O., Elobaid, E.A., Al-Obaidly, A., Al-Ansari, E., Philip Obbard, J.P., 2018. Baseline concentrations and distributions of Polycyclic Aromatic Hydrocarbons in surface sediments from the Qatar marine environment. Mar. Pollut. Bull. 126, 58–62.

Howells, E.J., Abrego, D., Meyer, E., Kirk, N.L., Burt, J.A., 2016. Host adaptation and unexpected symbiont partners enable reef-building corals to tolerate extreme temperatures. Glob. Chang. Biol. 22, 2702–2714.

Howells, E.J., Bauman, A.G., Vaughan, G.O., Hume, B.C.C., Voolstra, C.R., Burt, J.A., 2020. Corals in the hottest reefs in the world exhibit symbiont fidelity not flexibility. Mol. Ecol. 29, 899–911.

Kampf, J., Sadrinesab, M., 2006. The circulation of the Persian Gulf: a numerical study. Ocean Sci. 2, 27–41.

Kanamori, S., Ikegami, H., 1982. Calcium-alkalinity relationship in the North Pacific. J. Oceanogr. 38 (57–62), 1982.

Liss, P.S., Slater, P.G., 1974. Flux of Gases across the Air-Sea Interface. Nature 247, 181–184.

Lonborg, C., Calleja, M.L.I., Fabricius, K.E., Smith, J.N., Achterberg, E.P., 2019. The great barrier reef: A source of CO_2 to the atmosphere. Mar. Chem. 210, 24–33.

Lorenzen, C.J., 1967. Determination of chlorophyll and phaeopigments: spectrophotometric equations. Limnol. Oceanogr. 12, 343–346.

Millero, F.J., 2010. Carbonate constants for estuarine waters. Mar. Freshw. Res. 61, 139–142.

Mohammed, S.Z., Al-Ssadh, S., 1996. Coral reef grounds and its associated biota in the western side of the Arabian Gulf (ROPME sea area) with respect to 1991 Gulf War oil spill. Indian J Mar Sci 25, 35–40.

Orr, J.C., et al., 2005. Anthropogenic ocean acidification over the twenty-first century and its impact on calcifying organisms. Nature 437, 681–686. https://doi.org/10.1038/nature04095.

Orr, J.C., Epitalon, J.-M., Dickson, A.G., Gattuso, J.-P., 2018. Routine uncertainty propagation for the marine carbon dioxide system. Mar. Chem. 207, 84–107.

Pierrot, D., Lewis, E., Wallace, D.W.R., 2006. MS excel program developed for CO2 system calculations. In: ORNL/CDIAC-105a. Carbon Dioxide Information Analysis Center, Oak Ridge National Laboratory, U.S. Department of Energy, Oak Ridge, Tennessee. https://doi.org/10.3334/CDIAC/otg.CO2SYS_XLS_CDIAC105a.

Polikarpov, I., Saburova, M., Al-Yamani, F., 2016. Diversity and distribution of winter phytoplankton in the Arabian Gulf and the Sea of Oman. Cont. Shelf Res. 119, 85–99.

Quigg, A., Al-Ansi, M., Al Din, Nour, Wei, C.-L., Nunnally, C.C., Al-Ansari, I.S., Rowe, G. T., et al., 2013. Phytoplankton along the coastal shelf of an oligotrophic hypersaline environment in a semi-enclosed marginal sea: Qatar (Arabian Gulf). Cont. Shelf Res. 60, 1–16.

Radice, V.Z., Fry, B., Brown, K.T., Dove, S., Hoegh-Guldberg, O., 2022. Biogeochemical niches and trophic plasticity of shallow and mesophotic corals recovering from mass bleaching. Limnol. Oceanogr. 67, 1617–1630.

Rezai, H., Wilson, S., Claereboudt, M., Riegl, B., 2004. Coral reef status in the ROPME sea area: Arabian/Persian Gulf, Gulf of Oman and Arabian Sea. In: Wilkinson, C. (Ed.), Status of Coral Reefs of the World: 2004. Australian Institute of Marine Science, Townsville, pp. 155–169.

Romanó de Orte, M., Koweek, D.A., Cyronak, T., Takeshita, Y., Griffin, A., Wolfe, K., Szmant, A., Whitehead, R., Albright, R., Caldeira, K., 2021. Unexpected role of communities colonizing dead coral substrate in the calcification of coral reefs. Limnol. Oceanogr. 66, 1793–1803.

Saderne, V., Baldry, K., Anton, A., Agustí, S., Duarte, C.M., 2019. Characterization of the CO_2 system in a coral reef, a seagrass meadow, and a mangrove forest in the central Red Sea. J. Geophys. Res. Oceans 124, 7513–7528.

Shanableh, A., Al-Ruzouq, R., Gibril, M.B.A., Khalil, M.A., Al-Mansoori, S., Yilmaz, A.G., Imteaz, M.A., Flesia, C., 2021. Potential factors that trigger the suspension of calcium carbonate sediments and whiting in a semi-enclosed Gulf. Remote Sens. 13, 4795–4819.

Sheppard, C., Al-Husiani, M., Al-Jamali, F., Al-Yamani, F., Baldwin, R., Bishop, J., et al., 2010. The Gulf: a young sea in decline. Mar. Pollut. Bull. 60, 13–38.

Smith, S.V., Gattuso, J.-P., 2011. Balancing the oceanic calcium carbonate cycle: consequences of variable water column Ψ. Aquat. Geochem. 17, 327–337.

Smith, E.G., Hazzouri, K.M., Choi, J.Y., Delaney, P., Al-Kharafi, M., Howells, E.J., Aranda, M., Burt, J.A., 2022. Signatures of selection underpinning rapid coral adaptation to the world's warmest reefs. Sci. Adv. 8, eabl7287.

Spalding, M.D., et al., 2007. Marine ecoregions of the world: a bioregionalization of coastal and shelf areas. BioScience 57, 573–583.

Strickland, J.D.H., Parsons, T.R., 1972. A practical handbook of seawater analysis. Fisheries Research Board of Canada, Ottawa, p. 310.

Stumm, W., Morgan, J.J., 1995. Aquatic Chemistry: Chemical Equilibria and Rates in Natural Waters 3rd Edition. Wiley-Interscience, p. 1040.

Takahashi, T., et al., 2014. Climatological distributions of pH, pCO2, total CO2, alkalinity, and CaCO3 saturation in the global surface ocean, and temporal changes at selected locations. Mar. Chem. 164, 95–125.

Talley, L.D., et al., 2011. Descriptive Physical Oceanography: An Introduction, 6th. Elsevier.

Terlouw, G.J., Knor, L.A.C.M., De Carlo, E.H., Drupp, P.S., Mackenzie, F.T., Li, Y.H., Sutton, A.J., Plueddemann, A.J., Sabine, C.L., 2019. Hawaii coastal seawater CO2 network: a statistical evaluation of a decade of observations on tropical coral Reefs. Front. Mar. Sci. 6, 1–18. https://doi.org/10.3389/fmars.2019.00226.

Uddin, S., Gevao, B., Al-Ghadban, A.N., Nithyanandan, M., Al-Shamroukh, D., 2012. Acidification in Arabian Gulf-Insights from pH and temperature measurements. J. Environ. Monit. 14, 1479–1482.

Uppström, L.R., 1974. The boron/chlorinity ratio of deep-sea water from the Pacific Ocean. Deep-Sea Res. 21, 161–162.

Vaughan, G.O., Al-Mansoori, N., Burt, J.A., 2019. The Arabian Gulf. In: World Seas: An Environmental Evaluation. Elsevier, pp. 1–23. https://doi.org/10.1016/B978-0-08-100853-9.00001-4.

Wanninkhof, R., 1992. Relationship between wind speed and gas exchange over the ocean. J. Geophys. Res. 97, 7373–7382.

Wanninkhof, R., McGillis, W.R., 1999. A cubic relationship between air-sea CO_2 exchange and wind speed. Geophys. Res. Lett. 26, 1889–1892.

Ware, J.R., Smith, S.V., Reaka-Kudla, M.L., 1991. Coral reefs: sources or sinks of atmospheric CO_2? Coral Reefs 11, 127–130.
Williams, R.G., Follows, M.J., 2011. Ocean Dynamics and the Carbon Cycle. Cambridge University Press, New York, p. 404.
Wolf-Gladrow, D.A., Zeebe, R.E., Klaas, C., Koertzinger, A., Dickson, A.G., 2007. Total alkalinity: the explicit conservative expression and its application to biogeochemical processes. Mar. Chem. 106, 287–300.